

A Ternary Lattice Boltzmann Model for Amphiphilic Fluids

Hudong Chen

Exa Corporation,
Lexington, Massachusetts, U.S.A.
hudong@exa.com

Bruce M. Boghosian

Center for Computational Science,
Boston University, 3 Cummington Street, Boston, Massachusetts 02215, U.S.A.
bruceb@bu.edu

Peter V. Coveney

Centre for Computational Science,
Queen Mary and Westfield College, University of London,
Mile End Road, London E1 4NS, U.K.
p.v.coveney@qmw.ac.uk

September 3, 2018

Abstract

A lattice Boltzmann model for amphiphilic fluid dynamics is presented. It is a ternary model, in that it conserves mass separately for each chemical species present (water, oil, amphiphile), and it maintains an orientational degree of freedom for the amphiphilic species. Moreover, it models fluid interactions at the microscopic level by introducing self-consistent forces between the particles, rather than by positing a Landau free energy functional. This combination of characteristics fills an important need in the hierarchy of models currently available for amphiphilic fluid dynamics, enabling efficient computer simulation and furnishing new theoretical insight. Several computational results obtained from this model are presented and compared to existing lattice-gas model results. In particular, it is noted that lamellar structures, which are precluded by the Peierls instability in two-dimensional systems with kinetic fluctuations, are not observed in lattice-gas models, but are easily found in the corresponding lattice Boltzmann models. This points out a striking difference in the phenomenology accessible to each type of model.

Keywords: Amphiphilic fluids, fluid dynamics, lattice Boltzmann, lattice gas, microemulsions, Peierls instability

1 Introduction

Amphiphilic fluids consist of two immiscible phases, together with an amphiphile species that helps them to mix. A typical example is a mixture of oil and water with the addition of detergent. The molecules of detergent often have ionic “heads” that are hydrophylic, and hydrocarbon “tails” that are hydrophobic, and so there is a strong energetic preference for these to reside on the oil/water interface. Moreover, the presence of these orientable particles on the interface gives it a bending or curvature energy. These characteristics give amphiphilic fluids an extremely rich and complicated phenomenology, even in equilibrium. A wide variety of structures—including spherical and wormlike micelles, emulsion droplets, sponge phases and lamellae—can self-assemble on space and time scales that are very large in comparison with those of the component molecules, effectively ruling out molecular dynamics as a suitable methodology for studying such behaviour [1]. The addition of fluid dynamics and nontrivial rheology to such complicated equilibrium behaviour thus creates a very difficult problem indeed, but one with relevance to a wide variety of industrial, chemical and biological applications. These include oil recovery, pollution remediation, and the dynamics of vesicles and biomembranes, to name but a few.

Hydrodynamic lattice-gas automata (LGA) were first applied to *reduced* descriptions of amphiphilic fluids – in which the amphiphile species is modelled only by its effects on the surface properties of two immiscible phases [2]. To capture much of the above-described phenomenology, however, requires a *ternary vector model*, in which a separate amphiphile species possesses both translational and orientational degrees of freedom. Such models have been used to study the equilibrium properties of amphiphilic fluids for more than a decade now [3]. A few years ago, it was demonstrated that hydrodynamic LGA also provide an effective means of coupling the Hamiltonian of such vector models to hydrodynamic flow with conserved momentum, thereby providing a self-consistent treatment of the hydrodynamics of ternary amphiphilic fluids [4]. This model, which can also be regarded as an extension of Rothman and Keller’s immiscible-fluid algorithm [5] to include amphiphilic species, has been used to study the dynamics of phase separation [6], the shear-induced sponge-to-lamellar phase transition [7], and many other phenomena of amphiphilic fluid dynamics.

In the current work, we create a model of amphiphilic fluid dynamics that is based on a lattice Boltzmann (LB) model, rather than a LGA. Both models are kinetic in nature, and both have been implemented in both two and three dimensions [8], but the LB model is based on a single-particle distribution function, whereas the LGA is truly particulate. Phenomena that depend critically on kinetic fluctuations, nucleation and other particle discreteness effects are thus well described by the LGA model, but not by the LB model. On the other hand, the LB model is perfectly adequate for the treatment of bulk hydrodynamic phenomena, is simpler from an algorithmic point of view, and is more computationally efficient. Unlike the LGA model, which is far more complicated in three dimensions than in two owing to its use of lattice-specific many-body scattering processes, the LB model is easily implemented on lattices of any dimension.

In addition to introducing the new LB model, an important purpose of the present work is to understand its limitations relative to the LGA model. Along these lines, we shall focus on the self-assembly of lamellar phases in two and three dimensions. According to a very general theorem of Peierls [9, 10], in any infinite system with underlying kinetic fluctuations, thermodynamic equilibria that are periodic along one spatial dimension are necessarily unstable in two dimensions, but may be stable in three dimensions. Since the LB model lacks natural kinetic fluctuations, it may be expected to exhibit lamellae in two dimensions, and we present computer simulation evidence of this here. This situation stands in stark contrast to that for the corresponding LGA model, for which two dimensional lamellae have never been observed, presumably due to the Peierls instability.

2 Lattice Boltzmann Models of Hydrodynamics

LB models come in two varieties: So-called “top-down” models [11] assume an appropriate form for the free-energy, and assume that its approach to equilibrium is governed by a Ginzburg-Landau or Cahn-Hilliard equation; a LB collision operator is constructed that gives rise to the desired evolution equations in the hydrodynamic limit. “Bottom-up” models [12], by contrast, add particle interactions at the kinetic level, and so the form (indeed, even the existence) of the free energy, and the time-dependence of the approach to equilibrium are emergent properties of the large scale dynamics. Previous LB models of amphiphilic fluid dynamics have all been “top-down” in spirit, with a reduced description using one [13] or two [14] order parameters, but no surfactant orientational degrees of freedom. The present model, by contrast is ternary (it contains three species, although one can also consider any single or pairwise combination of components) and adopts a “bottom-up” approach, making it easier to compare to existing LGA vector models. More importantly, unlike either the LGA model or existing LB models, it offers complete control of the viscosities and molecular weights of the various species present. Indeed, the algorithm allows for any number of different species, including multiple types of amphiphiles, thus in principle enabling one to study *inter alia* the role of co-surfactants in these systems. This generality is evidently beneficial for studying a wider range of physico-chemical phenomena in amphiphilic fluids. Moreover, it has previously been argued that the current approach offers advantages of accuracy in the resulting hydrodynamic description [15].

A standard LB system involving multiple species is usually represented by a set of finite difference equations [16, 17],

$$n_i^\sigma(\mathbf{x} + \hat{\mathbf{c}}_i, t + 1) - n_i^\sigma(\mathbf{x}, t) = \Omega_i^\sigma \quad i = 0, 1, \dots, b, \quad (1)$$

where $n_i^\sigma(\mathbf{x}, t)$ is the single-particle distribution function, indicating the amount of species σ (indicating, *e.g.*, oil, water or amphiphile), having velocity $\hat{\mathbf{c}}_i$, at site \mathbf{x} on a D -dimensional lattice of coordination number b , at time step t . The collision operator Ω_i^σ represents the change in the single-particle distribution function due to collisions. In the absence of chemical reactions, this operator must conserve the mass of *each* species,

$$\sum_i m_\sigma \Omega_i^\sigma = 0, \quad (2)$$

where m_σ is the molecular weight for species σ . Likewise, in the absence of external forces, it must also conserve the momentum of *all* the species,

$$\sum_\sigma \sum_i m_\sigma \hat{\mathbf{c}}_i \Omega_i^\sigma = 0. \quad (3)$$

In the present work, we suppose that the system’s microscopic degrees of freedom are attached to a heat bath at fixed temperature T , so that there is no corresponding requirement for energy conservation.

For convenience, a “BGK” form [18] is often chosen for the collision operator,

$$\Omega_i^\sigma = -\frac{1}{\tau_\sigma} (n_i^\sigma - n_i^{\sigma\text{eq}}), \quad (4)$$

where the equilibrium distribution function is constructed to satisfy certain desiderata, including the required conservation conditions [19, 20]. Most LB models adopt a polynomial form for this equilibrium distribution function, such as

$$n_i^{\sigma\text{eq}} = g_i n^\sigma \left[1 + \beta_0 \hat{\mathbf{c}}_i \cdot \tilde{\mathbf{u}} + \frac{1}{2} \beta_0^2 (\hat{\mathbf{c}}_i \cdot \tilde{\mathbf{u}})^2 - \beta_0 \frac{\tilde{u}^2}{2} + \frac{1}{6} \beta_0^3 (\hat{\mathbf{c}}_i \cdot \tilde{\mathbf{u}})^3 - \beta_0^2 \frac{\tilde{u}^2}{2} (\hat{\mathbf{c}}_i \cdot \tilde{\mathbf{u}}) \right], \quad (5)$$

where $n^\sigma \equiv \sum_i n_i^\sigma$, and where the degeneracy constants g_i and the constant β_0 are specified entirely by the choice of lattice. For example, $\beta_0 = 3$ for the so-called D3Q19 lattice [20, 21] in three dimensions with 19 states. In Eq. (5) we have defined

$$\tilde{\mathbf{u}} = \frac{\sum_\sigma \frac{\rho^\sigma \mathbf{u}^\sigma}{\tau_\sigma}}{\sum_\sigma \frac{\rho^\sigma}{\tau_\sigma}} \quad (6)$$

where $\rho^\sigma = m_\sigma n^\sigma$ and $\rho^\sigma \mathbf{u}^\sigma = m_\sigma \sum_i \hat{\mathbf{c}}_i n_i^\sigma$. Such a form for the equilibrium distribution ensures that the local mass and momentum values are collisionally invariant [22]. Indeed, one can directly verify that

$$\sum_i n_i^\sigma = \sum_i \tilde{n}_i^\sigma, \quad \forall \sigma$$

and

$$\sum_\sigma \sum_i m_\sigma \hat{\mathbf{c}}_i n_i^\sigma = \sum_\sigma \sum_i m_\sigma \hat{\mathbf{c}}_i \tilde{n}_i^\sigma, \quad (8)$$

where

$$\tilde{n}_i^\sigma \equiv n_i^\sigma + \Omega_i^\sigma = n_i^\sigma - \frac{1}{\tau_\sigma} (n_i^\sigma - n_i^{\sigma \text{eq}}) \quad (9)$$

is the post-collision distribution. The choice of $n_i^{\sigma \text{eq}}$ then results in Navier-Stokes hydrodynamics, where each component σ has viscosity $\nu^\sigma = (\tau_\sigma - 1/2)/\beta_0$.

3 Immiscible Lattice Boltzmann Model

Immiscibility of two or more species is modelled by introducing a discrete realization of the self-consistently generated mean-field body force between the particles [12]. Without an amphiphilic species, and considering only nearest-neighbour interactions among the immiscible species $\sigma \in \{1, \dots, \sigma_m\}$, the simplest possible form for such a force is

$$\mathbf{F}^{\sigma,c}(\mathbf{x}, t) = -\psi^\sigma(\mathbf{x}, t) \sum_{\bar{\sigma}} \sum_i g_{\sigma\bar{\sigma}} \psi^{\bar{\sigma}}(\mathbf{x} + \hat{\mathbf{c}}_i, t) \hat{\mathbf{c}}_i, \quad (10)$$

where the parameter $g_{\sigma\bar{\sigma}}$ (positive for repulsive forces, negative for attractive ones) represents the interaction strength between the two components, σ and $\bar{\sigma}$. Here we have introduced the *effective charge* ψ^σ , which can be chosen to be any suitable function of the local mass density ρ^σ , as appropriate for the force laws of the hydrodynamic system of interest. The dynamical effect of the force is realised in the BGK collision operator in Eq. (4) by adding to the velocity $\tilde{\mathbf{u}}$, in the equilibrium distribution $n_i^{\sigma \text{eq}}$ of Eq. (5), an increment

$$\delta \mathbf{u}^\sigma = \tau_\sigma \mathbf{F}^{\sigma,c} / \rho^\sigma. \quad (11)$$

This procedure has recently been shown to be systematically derivable from the body-force term of the standard continuum Boltzmann equation, based on a Hermite moment expansion [23]. Indeed, with this algorithm, phase separation has been demonstrated for sufficiently large values of $g_{\sigma\bar{\sigma}}$ [12, 24]. It is worthwhile to point out that, although the overall momentum change at any given lattice site and time may be non-zero,

$$\mathbf{F}(\mathbf{x}, t) = \sum_\sigma \mathbf{F}^{\sigma,c}(\mathbf{x}, t) = \sum_\sigma \rho^\sigma(\mathbf{x}, t) \delta \mathbf{u}^\sigma(\mathbf{x}, t), \quad (12)$$

Newton's third law, and hence global momentum conservation, is satisfied exactly by Eq. (10),

$$\sum_{\mathbf{x}} \mathbf{F}(\mathbf{x}, t) = 0. \quad (13)$$

4 Amphiphilic Lattice Boltzmann Model

With the addition of amphiphile, the LB Eqs. (1), (4), (5) and (11) remain unchanged, and the species label σ simply extends to include the amphiphile species s . Although as noted above the basic algorithm is general enough to treat multiple amphiphile species, for simplicity here we consider only a single type of amphiphile. Incorporation of the physics of amphiphilic fluid particles requires two fundamentally new types of body forces, in addition to those described above. Unlike ordinary species such as oil and water, which can be approximated by point (or spherical) particles so that their interactions depend on relative distances alone, the essential character of an amphiphilic molecule is more appropriately represented by a dipole; their interactions depend not only on their relative distances but also on their dipolar orientations [4]. It is these additional fundamental features which result in all the fascinating phenomenology described in the Introduction.

We first introduce an average dipole vector $\mathbf{d}(\mathbf{x}, t)$ at each site \mathbf{x} to represent the orientation of any amphiphile present there. The direction of this dipole vector is allowed to vary continuously in the present model (although we could do so, we do not attempt to discretise the dipolar orientation here). We assume that the dipole vector for a single amphiphile molecule has magnitude \hat{d}_0 , and we suppose that there are N amphiphile molecules represented by a single lattice-gas particle, so that $|\mathbf{d}(\mathbf{x}, t)| \leq d_0 \equiv N\hat{d}_0$, where equality holds if and only if all the amphiphile molecules are perfectly aligned. Note that the model does not specify dipole information for each velocity $\hat{\mathbf{c}}_i$, for reasons of computational efficiency and simplicity; information on the average dipole direction at each site is adequate for the present model. The propagation of $\mathbf{d}(\mathbf{x}, t)$ can then be defined by the simple relation,

$$n^s(\mathbf{x}, t + 1)\mathbf{d}(\mathbf{x}, t + 1) = \sum_i \tilde{n}_i^s(\mathbf{x} - \hat{\mathbf{c}}_i, t)\tilde{\mathbf{d}}(\mathbf{x} - \hat{\mathbf{c}}_i, t). \quad (14)$$

Note that the *dynamics* of the flow is entirely contained in the distribution function $\tilde{n}_i^s(\mathbf{x} - \hat{\mathbf{c}}_i, t)$. In Eq. (14), $\tilde{\mathbf{d}}$ represents the post-collision average dipole vector per site, whose relaxation is also governed by a BGK process,

$$\tilde{\mathbf{d}}(\mathbf{x}, t) = \mathbf{d}(\mathbf{x}, t) - \frac{1}{\tau_d} [\mathbf{d}(\mathbf{x}, t) - \mathbf{d}^{\text{eq}}(\mathbf{x}, t)] \quad (15)$$

with τ_d representing relaxation of a dipole vector to a local equilibrium $\mathbf{d}^{\text{eq}}(\mathbf{x}, t)$. Eqs. (14) and (15) completely determine the evolution of the dipoles once an explicit expression for $\mathbf{d}^{\text{eq}}(\mathbf{x}, t)$ is specified. Furthermore, it can be seen that the magnitude of the dipole vector is guaranteed to be less than d_0 at all times if $\tau_d \geq 1$ and $|\mathbf{d}^{\text{eq}}| \leq d_0$.

Unlike momentum vectors, there is no conservation requirement associated for the dipole vectors. On the other hand, their direction and magnitude are affected by the distribution of the other dipoles as well as of oil and water molecules in their neighbourhood. It is physically reasonable to assume that the local equilibrium at a given site is the same for all amphiphile molecules, regardless of their velocity values. That is, if we let $\mathbf{d}_i^{\text{eq}}(\mathbf{x}, t)$ be the equilibrium dipole value for amphiphiles of velocity $\hat{\mathbf{c}}_i$, then

$$\mathbf{d}_i^{\text{eq}}(\mathbf{x}, t) = \mathbf{d}^{\text{eq}}(\mathbf{x}, t), \quad \forall i. \quad (16)$$

Moreover, such an equilibrium property should not depend on the history of the dipole distribution. Both the orientation and magnitude of the equilibrium dipole vector are dictated by the nature

of the particles in its neighbourhood and so one of most appropriate choices is to use the Gibbs measure:

$$\mathbf{d}^{\text{eq}}(\mathbf{x}, t) = d_0 \frac{\sum_{\alpha} e^{-\beta H_{\alpha}(\mathbf{x}, t)} \hat{\phi}_{\alpha}}{\sum_{\alpha} e^{-\beta H_{\alpha}(\mathbf{x}, t)}} \quad (17)$$

where $\hat{\phi}_{\alpha}$, for $\alpha \in \{1, \dots, W\}$ are a set of unit vectors representing all possible dipole orientations. Obviously, Eq. (17) ensures $|\mathbf{d}^{\text{eq}}| \leq d_0$. The parameter $\beta = 1/T$ represents the inverse of the temperature of the aforementioned heat bath, with which the microscopic relaxation process is assumed to be in contact. From Eq. (17), one can immediately make the interpretation that the dipole tends to align itself in the direction which minimizes the energy, H_{α} . If we consider the dipoles' vector interactions, it is plausible to assume the following form for H_{α} , which can be interpreted as a generalization of the Heisenberg model Hamiltonian in magnetism,

$$H_{\alpha}(\mathbf{x}, t) = -\hat{\phi}_{\alpha} \cdot \mathbf{h}(\mathbf{x}, t) \quad (18)$$

where

$$\mathbf{h}(\mathbf{x}, t) = \mathbf{h}^s(\mathbf{x}, t) + \mathbf{h}^c(\mathbf{x}, t) \quad (19)$$

is a mean field created by the surrounding distributions. Its two contributions, $\mathbf{h}^s(\mathbf{x}, t)$ and $\mathbf{h}^c(\mathbf{x}, t)$, are associated with distributions of ordinary species and amphiphiles, respectively. If we consider only nearest-neighbour interactions for simplicity, these vector fields have the following forms

$$\mathbf{h}^c(\mathbf{x}, t) = \sum_{\sigma} e_{\sigma} \sum_i n^{\sigma}(\mathbf{x} + \hat{\mathbf{c}}_i, t) \hat{\mathbf{c}}_i \quad (20)$$

where e_{σ} (which may, for example, take its values from the set $\{-e, 0, +e\}$ where e is constant) is the *colour charge* (order parameter) for ordinary species. This form may be interpreted physically as a discrete approximation of the colour gradient of the immiscible species. Similarly, we have

$$\mathbf{h}^s(\mathbf{x}, t) = \sum_i \left[\sum_{j \neq 0} n_i^s(\mathbf{x} + \hat{\mathbf{c}}_j, t) \boldsymbol{\theta}_j \cdot \mathbf{d}_i(\mathbf{x} + \hat{\mathbf{c}}_j, t) + n_i^s(\mathbf{x}, t) \mathbf{d}_i(\mathbf{x}, t) \right], \quad (21)$$

where we have defined the traceless second-rank tensor

$$\boldsymbol{\theta}_j \equiv \mathbf{I} - D \frac{\hat{\mathbf{c}}_j \hat{\mathbf{c}}_j}{c^2}, \quad (22)$$

and where in turn \mathbf{I} is the second-rank unit tensor and D the spatial dimension. The physical reason for the appearance of the tensor $\boldsymbol{\theta}_j$ is that dipoles tend to align when their relative positions are orthogonal to their mean dipolar orientation (*i.e.*, $\mathbf{d} \cdot \hat{\mathbf{c}}_j = 0$), and anti-align when these are parallel. Since we let $\hat{\phi}_{\alpha}$ take on continuous values, in three dimensions Eq. (17) can be integrated analytically to give

$$\mathbf{d}^{\text{eq}} = d_0 \left[\coth(\beta h) - \frac{1}{\beta h} \right] \hat{\mathbf{h}} \quad (23)$$

which becomes

$$\mathbf{d}^{\text{eq}} \approx d_0 \frac{\beta h}{3} \hat{\mathbf{h}} \quad (24)$$

in the limit of small βh . Here we have defined the unit vector $\hat{\mathbf{h}} \equiv \mathbf{h}(\mathbf{x}, t)/|\mathbf{h}(\mathbf{x}, t)|$, and magnitude $h \equiv |\mathbf{h}(\mathbf{x}, t)|$.

With the presence of an amphiphilic species s , the force on an oil or water particle σ needs to include an additional term

$$\mathbf{F}^{\sigma}(\mathbf{x}, t) = \mathbf{F}^{\sigma, c}(\mathbf{x}, t) + \mathbf{F}^{\sigma, s}(\mathbf{x}, t), \quad (25)$$

where $\mathbf{F}^{\sigma,c}$ is just the original contribution from the ordinary molecules given by Eq. (10); the second term in Eq. (25) is the contribution from nearby amphiphiles whose specific form can be derived directly from a leading-order expansion of Eq. (10). To see how this latter expression may be derived, recall that an amphiphilic molecule possesses a hydrophilic (positive colour) head and a hydrophobic (negative colour) tail. Such a *colour dipole* can be modelled by a pair of oppositely (colour) charged fictitious particles with locations displaced by $\pm\mathbf{d}/2$ from the molecular center of mass location \mathbf{x} . On this basis, we can derive an analytical form for the resulting force from Eq. (10) via a Taylor expansion in \mathbf{d} . When only nearest-neighbour interactions are considered, the form of this interaction is given by

$$\mathbf{F}^{\sigma,s}(\mathbf{x}, t) = -2\psi^\sigma(\mathbf{x}, t)g_{\sigma s} \sum_{i \neq 0} \tilde{\mathbf{d}}(\mathbf{x} + \hat{\mathbf{c}}_i, t) \cdot \boldsymbol{\theta}_i \psi^s(\mathbf{x} + \hat{\mathbf{c}}_i, t), \quad (26)$$

where the parameter $g_{\sigma s}$ is the coupling coefficient between an ordinary and an amphiphilic species.

Using similar physical arguments, we can derive the forces on amphiphilic particles,

$$\mathbf{F}^s(\mathbf{x}, t) = \mathbf{F}^{s,c}(\mathbf{x}, t) + \mathbf{F}^{s,s}(\mathbf{x}, t), \quad (27)$$

where $\mathbf{F}^{s,c}$ and $\mathbf{F}^{s,s}$ represent forces from ordinary species and amphiphiles, respectively. In similar fashion, explicit forms for both of these forces can be derived directly from the force law, Eq. (10), for ordinary immiscible species; physically, the force $\mathbf{F}^{s,c}$ is simply the reaction force to $\mathbf{F}^{\sigma,s}$. It may be shown to have the following form,

$$\mathbf{F}^{s,c}(\mathbf{x}, t) = 2\psi^s(\mathbf{x}, t)\tilde{\mathbf{d}}(\mathbf{x}, t) \cdot \sum_{\sigma} g_{\sigma s} \sum_{i \neq 0} \boldsymbol{\theta}_i \psi^\sigma(\mathbf{x} + \hat{\mathbf{c}}_i, t), \quad (28)$$

from which we can verify that Newton's third law is satisfied,

$$\sum_{\mathbf{x}} \left[\sum_{\sigma} \mathbf{F}^{\sigma,s}(\mathbf{x}, t) + \mathbf{F}^{s,c}(\mathbf{x}, t) \right] = 0. \quad (29)$$

To the leading order of a Taylor expansion in the ratio of $|\mathbf{c}_i|$ to the colour gradient scale length, Eqs. (26) and (28) reduce to

$$\mathbf{F}^{\sigma,s}(\mathbf{x}) = -\frac{2bc^2}{D(D+2)}g_{\sigma s}\psi^\sigma(\mathbf{x}) \left\{ \nabla^2 \left[\tilde{\mathbf{d}}(\mathbf{x})\psi^s(\mathbf{x}) \right] - D\nabla\nabla \cdot \left[\tilde{\mathbf{d}}(\mathbf{x})\psi^s(\mathbf{x}) \right] \right\} \quad (30)$$

and

$$\mathbf{F}^{s,c}(\mathbf{x}) = \frac{2bc^2}{D(D+2)}g_{\sigma s}\psi^s(\mathbf{x})\tilde{\mathbf{d}}(\mathbf{x}) \cdot \sum_{\sigma} \left[\mathbf{I}\nabla^2\psi^\sigma(\mathbf{x}) - D\nabla\nabla\psi^\sigma(\mathbf{x}) \right]. \quad (31)$$

The above expressions make manifest the physically reasonable result that fluid particles experience no net force if the other particles in their neighborhood are distributed uniformly. More interesting is the result that the leading-order contributions involve second-order spatial derivatives. This implies that amphiphiles tend to reside near the interface between two immiscible fluids.

Finally, $\mathbf{F}^{s,s}$ represents the force due to interactions between amphiphilic particles. This depends not only on the relative distance but also on the relative orientation of the dipoles in question. Though considerably more involved algebraically, its expression is still derivable from small expansions of the polarization \mathbf{d} about \mathbf{x} as well as those at the neighbouring sites, as described above.

In particular, when only nearest-neighbour interactions are considered, this force has the simple form

$$\begin{aligned} \mathbf{F}^{s,s}(\mathbf{x}) = & -\frac{4D}{c^2}g_{ss}\psi^s(\mathbf{x})\sum_i\left\{\tilde{\mathbf{d}}(\mathbf{x}+\hat{\mathbf{c}}_i)\cdot\boldsymbol{\theta}_i\cdot\tilde{\mathbf{d}}(\mathbf{x})\hat{\mathbf{c}}_i\right. \\ & \left. + \left[\tilde{\mathbf{d}}(\mathbf{x}+\hat{\mathbf{c}}_i)\tilde{\mathbf{d}}(\mathbf{x}) + \tilde{\mathbf{d}}(\mathbf{x})\tilde{\mathbf{d}}(\mathbf{x}+\hat{\mathbf{c}}_i)\right]\cdot\hat{\mathbf{c}}_i\right\}\psi^s(\mathbf{x}+\hat{\mathbf{c}}_i). \end{aligned} \quad (32)$$

Here the coupling coefficient g_{ss} should be negative if we wish to model attraction between two amphiphile heads and repulsion between a head and a tail. Likewise, it can be verified directly that global momentum conservation is satisfied by this form; that is,

$$\sum_{\mathbf{x}}\mathbf{F}^{s,s}(\mathbf{x},t)=0, \quad (33)$$

when boundary effects are absent.

To summarize, the basic LB evolution equation is given by Eq. (1). The BGK operator for collisional relaxation is given by Eq. (4), where the collisional equilibrium is given by Eq. (5); this describes an ordinary LB algorithm for miscible Navier-Stokes fluids. To realise immiscibility, we implement the force, Eq. (10), between neighbouring particles by shifting the velocity used in Eq. (5) by the amount specified in Eq. (11); this describes the previously known ‘‘bottom-up’’ immiscible fluid LB algorithm. The principal contribution of this work is the introduction of a surfactant species with an orientation that propagates according to Eq. (14), and relaxes according to the BGK-like orientational collision operator, Eq. (15), with orientational equilibrium given by Eqs. (23), (20) and (21). The force on ordinary oil/water species due to amphiphile is given by Eq. (26), that on amphiphile due to ordinary species is given by Eq. (28), and that on amphiphile due to other amphiphile is given by Eq. (32). The effect of these forces on the collisional relaxation is also treated by shifting the velocity used in the BGK equilibrium by an amount specified in Eq. (11). Taken together, these equations completely specify the new ternary amphiphilic LB model and associated algorithm.

5 Simulations

In this section we demonstrate qualitatively that some of the basic phenomenology of amphiphilic fluids is indeed exhibited by the new model. We begin by verifying that the model with the amphiphilic interactions extinguished displays complete oil-water phase separation. All simulations shown in this section were performed on a domain of size 32×32 lattice units with periodic boundary conditions, and used $\tau_\sigma = \tau_s = \tau_d = 1$ and $\beta = 10$.

Fig. 1 shows the equilibrated colour order parameter at 6000 and 16000 time steps after an off-critical quench. The run began with blue density $\bar{n}^b = 0.45$, red density $\bar{n}^r = 0.65$ and surfactant density $\bar{n}^s = 0.25$, distributed homogeneously in space, aside from a small random fluctuation. For sufficiently strong interaction parameter ($g_{br} = 0.03$ was used here) between the immiscible red and blue phases, complete separation was observed as can be seen in the figure. Because the amphiphile interaction parameters were turned off ($g_{bs} = g_{ss} = 0$), the separation did not arrest, and the blue fluid formed a single droplet (recall that the boundary conditions are periodic).

Next, using the same density values and initial conditions as above, but with the amphiphilic interactions switched on ($g_{bs} = g_{ss} = -0.01$), Fig. 2 shows the colour order parameter and the surfactant director density after 16000 time steps, by which time the system appears to be in a stationary state. Note that the amphiphile has organised itself on the surface, with directors pointing from blue to red on average. This effectively demonstrates that the amphiphile has arrested

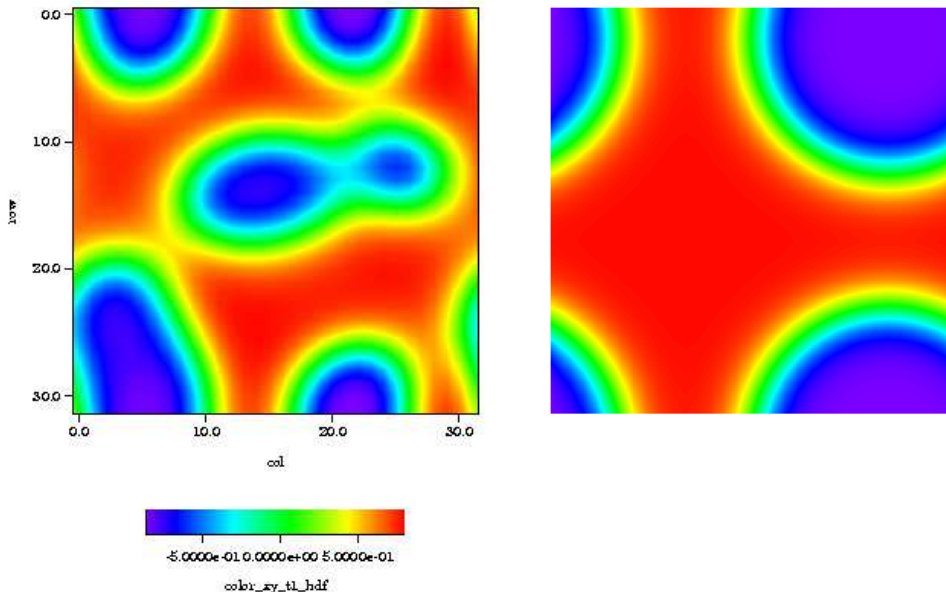


Figure 1: Two-dimensional binary oil(red)-water(blue) phase separation. Colour (oil-water) distributions shown at lattice timesteps $t = 6000$ (left) and $t = 16000$ (right)

the phase separation; if the separation were to continue, there would not be sufficient surface area to accommodate the amphiphile, which incurs a large energy penalty for being away from a surface. Such arresting of domain growth has previously been observed in LGA studies of amphiphilic fluids [6].

Fig. 3 shows the equilibrated colour order parameter and director density, 20000 time steps after a critical quench on a domain of size 32×32 lattice units. The run began with $\bar{n}^b = \bar{n}^r = 0.5$ and $\bar{n}^s = 0.1$, distributed homogeneously in space, aside from a small random fluctuation. No further evolution of the order parameter was observed after a few thousand time steps, strengthening the case that this is indeed an equilibrium state.

6 Discussion and Conclusions

As mentioned in the Introduction, an important focus of our studies to date with the new model has centered on the question of the existence of lamellae in two spatial dimensions. The theorem that we invoke was derived by Peierls in the context of electronic structure [9, 10], but is general enough to apply here. Let us suppose that a structure $\phi(x)$ that is periodic along dimension x minimizes some free energy functional $F[\phi]$. Let us further suppose that this structure undergoes thermally induced fluctuations in a Gibbsian distribution $\exp(-\delta F/T)$, where δF is the free energy excess due to the fluctuation. Peierls demonstrated that the variance of the component of such fluctuations in the direction of the periodicity is proportional to

$$T \int \frac{dk_x k_{\perp} dk_{\perp}}{\phi(k_x, k_{\perp}^2)}, \quad (34)$$

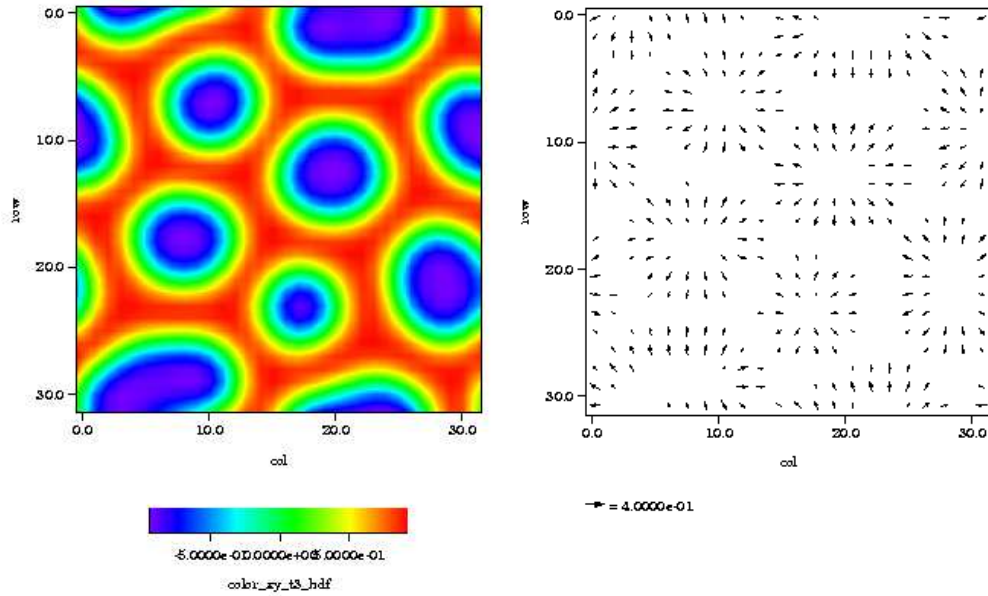


Figure 2: Two-dimensional domain growth in a ternary (oil-water-surfactant) fluid. Colour (oil-water, left) and amphiphile director (right) distributions are both shown at lattice timestep $t = 16000$

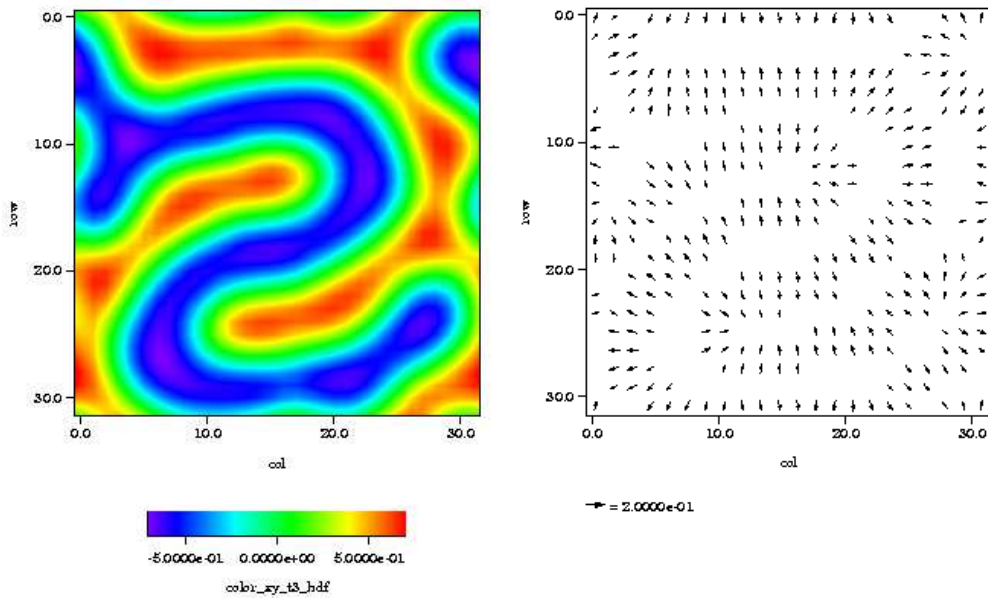


Figure 3: Formation of a lamellar phase in a ternary oil-water surfactant lattice Boltzmann fluid. Colour (left) and amphiphile (right) distribution are shown, both at lattice timestep $t = 20000$

where ϕ is an analytic function of its arguments that vanishes when its arguments are zero. This variance is easily seen to diverge logarithmically for small wavevector (large system size) for any finite temperature $T > 0$. Moreover, similar arguments show that such a divergence does not occur in three spatial dimensions.

Thus, we should expect lamellar structures to be unstable in an infinite two dimensional system with finite-temperature fluctuations. Indeed, previous lattice-gas studies of amphiphilic fluids in two dimensions [4, 7] have not found stable lamellae, despite extensive parametric searches for them, except when the system was sheared [7]. Lattice-gas studies in three dimensions, however, do exhibit stable unsheared lamellar structures [8]. We suggest here that the observed instability of lamellae in two dimensions is due to the Peierls mechanism. However, we must qualify this claim with the proviso that it is somewhat dangerous to assume that the Peierls instability applies in a lattice-gas simulation: although a LGA is indeed a finite-temperature, fluctuating system, computer simulations of it always have a finite domain size, and hence a minimum sustainable wavevector. This objection might be mitigated if it could be shown that lamellar phases reappear at zero temperature. Unfortunately, it is impossible to lower the effective temperature of a LGA to zero; kinetic fluctuations will always be present by the very nature of the model. LB methods, by contrast, have no kinetic fluctuations. Thus, if an LB model were to exhibit lamellae in two dimensions, it would strengthen the argument that their absence in the LGA model is due to the Peierls instability. As described in the previous section, we tested this by simulating the critical quench shown in Fig. 3; that this resulted in a lamellar phase supports the above interpretation of the Peierls instability.

In conclusion, we have described a ternary lattice Boltzmann model of amphiphilic fluids. This model differs from previous LB models in that it accounts for amphiphilic director orientation, and incorporates microscopic interactions between the fluid particles, without the need to postulate a free energy functional. It differs from LGA models in that it does not include fluctuations associated with particle discreteness. The lack of fluctuations gives the model a different phase behaviour from the corresponding LGA; in particular, we have presented evidence from computer simulation that it exhibits lamellar phases in two dimensions, which are prohibited by the Peierls instability in models with fluctuations.

Acknowledgements

The authors would like to thank Ye Zhou for his help with coding an earlier version of the model. The authors' collaboration was facilitated by a travel grant from NATO (grant number CRG950356). BMB was supported in part by the United States Air Force Office of Scientific Research under grant number F49620-95-1-0285, and in part by AFRL.

References

- [1] J-B. Maillet, V. Lachet and P.V. Coveney "Large scale molecular dynamics simulation of self-assembly processes in short and long chain cationic surfactants", *Phys. Chem. Chem. Phys.*, **1** (1999), in press.
- [2] S-Y. Chen, T. Lookman, *J. Stat. Phys.*, **81**, 223-235 (1995).
- [3] G. Gompper, M. Schick, *Phase Transitions and Critical Phenomena*, **16** (1994) 1-181.
- [4] B. Boghosian, P. Coveney, and A. Emerton, *Proc. R. Soc. Lond. A*, **452**, 1221 (1996).

- [5] D. H. Rothman and J. M. Keller, *J. Stat. Phys.*, **52**, 1119 (1988); A. K. Gunstensen, D. H. Rothman, S. Zaleski, and G. Zanetti, *Phys. Rev. A*, **43**, 4320 (1991).
- [6] A.N. Emerton, P.V. Coveney, B.M. Boghosian, *Phys. Rev. E*, **55**, 708-720 (1997).
- [7] A.N. Emerton, F.W.J. Weig, P.V. Coveney, B.M. Boghosian, *J. Phys. Condens. Mat.*, **9** 8893-8905 (1997).
- [8] B.M. Boghosian, P.V. Coveney and P.J. Love, "Three-dimensional lattice-gas model for amphiphilic fluid dynamics", *Proc. R. Soc. London A*, in press (1999).
- [9] R.E. Peierls, "Quantum Theory of Solids," Clarendon Press, Oxford University (1955).
- [10] L.D. Landau and E.M. Lifshitz, "Statistical Physics, Part I," Butterworth Heinemann (1997), pp. 432-436.
- [11] M. Swift, W. Osborn and J. Yeomans, *Phys. Rev. Lett.*, **75**, 830 (1995); M. Swift, S. Orlandini, W. Osborn and J. Yeomans, *Phys. Rev. E*, **54**, 5041 (1996).
- [12] X. Shan and H. Chen, *Phys. Rev. E*, **47**, 1815 (1993); X. Shan and H. Chen, *Phys. Rev. E*, **49**, 2941 (1994).
- [13] O. Theissen, G. Gompper and D.M. Kroll, *Europhys. Lett.*, **42**, 419 (1998).
- [14] G. Gonella, E. Orlandini and J.M. Yeomans, *Phys. Rev. Lett.*, **78**, 1695 (1997); A. Lamura, G. Gonella and J.M. Yeomans, *Int. J. Mod. Phys. C*, **9**, 1469 (1998).
- [15] X. He, X. Shan, and G. Doolen, *Phys. Rev. E*, **57**, R13 (1998).
- [16] F. Higuera, S. Succi and R. Benzi, *Europhys. Lett.*, **9**, 345 (1989); and R. Benzi, S. Succi and M. Vergassola, *Physics Reports*, **222**, 145 (1992).
- [17] S. Chen and G. Doolen, *Ann. Rev. Fluid Mech*, **30**, 329 (1998).
- [18] P. Bhatnagar, E. Gross and M. Krook, *Phys. Rev.*, **94**, 511 (1954).
- [19] S. Chen, H. Chen, D. Martinez and W. Matthaeus, *Phys. Rev. Lett.*, **67**, 3776 (1991); H. Chen, S. Chen and W. Matthaeus, *Phys. Rev. A*, **45**, 5339 (1992).
- [20] Y. Qian, D. d'Humières and P. Lallemand, *Europhys. Lett.*, **17**, 479 (1992).
- [21] U. Frisch, D. D'Humieres, B. Hasslacher, P. Lallemand, Y. Pomeau, and J. Rivet, *Complex Systems*, **1**, 649 (1987).
- [22] X. Shan and G. Doolen, *J. Stat. Phys.*, **81**, 379 (1995).
- [23] N. Martys, X. Shan, and H. Chen, *Phys. Rev. E*, **58**, 6855 (1998).
- [24] N. Martys and H. Chen, *Phys. Rev. E*, **53**, 743 (1995).